I^-. Disproportionation of I_2^- (eq 6) occurs with a rate constant of 8×10^9 M^{-1} s^{-1}; thus, the metastable products of flash irradiation would be $Ru(NH_3)_5py^{2+}$ plus I_3^-. The slow second-order relaxation of these species apparently reflects the relatively small rate constant of eq 7. Preliminary stopped-flow experiments of this redox reaction confirmed the approximate rate of this reaction although, as in the case of the flash experiments, the relatively intense light source used in the stopped-flow spectrometer led to photocatalysis and precluded an accurate measurement of the rate constant. Such photocatalysis probably involves the light-driven reverse of eq 6 since I_3^- absorbs at the monitoring wavelengths 400 nm. Preliminary pulse radiolysis experiments have demonstrated a second-order rate constant of 2.3×10^9 M^{-1} s^{-1} for eq 8.[17]

The strongly absorbing transients observed in the laser flash photolysis of the Ru(III)/Br^- solutions very likely are the result of the formation of Ru(II) plus Br_2^-. The very fast ($k_9 = 5 \times 10^{10}$ M^{-1} s^{-1}) relaxation of these solutions back to starting materials apparently reflects eq 9, which has a driving force

$$\mathrm{Ru(NH_3)_5py^{2+} + Br_2^- \xrightarrow{k} Ru(NH_3)_5py^{3+} + 2Br^-} \quad (9)$$

even larger than that of eq 8. The failure to see any transients for the analogous laser flash photolysis with the $Ru(NH_3)_5py^{3+}/Cl^-$ solutions is the probable result of two factors. One would be the lower sensitivity of this experiment resulting from the necessity to use a less intense pulse of shorter wavelength; the second would be the even faster rates in this case for relaxation processes such as the analogues of k_{-4} and k_8.

In summary, the flash photolysis studies described here demonstrate that the principal photochemical result of OSLMCT excitation of the ion pairs $Ru(NH_3)_5py^{3+}/X^-$ (X = I or Br) is the formation of ruthenium(II) transients that relax to starting materials via second-order reactions with the resulting oxidized halogen species. If the counterion is an irreversible reductant (e.g. $C_2O_4^{2-}$), such photolysis can lead to substantial net photoreduction of the metal center under continuous photolysis. For the halides, CW photolysis of the OSLMCT absorptions leads only to modest photosubstitution of the Ru(III) coordination sphere with quantum yields comparable to those for $Ru(NH_3)_5py^{3+}$ in dilute perchlorate solutions. However, for X = I substantially higher ϕ_{NH_3} and ϕ_{py} values are noted, a result that suggests some special reactivity of the OSLMCT state in this case. In this context, we consider an attractive speculation to be that relaxation of species A via the k_{-4} pathway might occur in part via an "inner-sphere" reaction between the electrophile I· and the electron-rich $Ru(NH_3)_5py^{2+}$ ion, giving a seven-coordinate Ru(II) intermediate $[Ru(NH_3)_5(py)I]^{2+}$, which can relax to the normal six-coordinate state by loss of I^-, NH_3, or py.

Acknowledgment. This research was supported by the National Science Foundation. Ruthenium used in these investigations was provided on loan by Johnson-Matthey Inc.

Registry No. $Ru(NH_3)_5py^{3+}$, 33291-25-7; $Ru(NH_3)_5py^{2+}$, 21360-09-8; $Ru(NH_3)_5(H_2O)^{3+}$, 25590-52-7; $Ru(NH_3)_4(H_2O)py^{3+}$, 88034-44-0; Cl^-, 16887-00-6; Br^-, 24959-67-9; I^-, 20461-54-5; $C_2O_4^{2-}$, 338-70-5; I_3^-, 14900-04-0.

---

[17] Cohen, H.; private communication.

Contribution from the Departments of Chemistry and Chemical Engineering,
Virginia Polytechnic Institute and State University, Blacksburg, Virginia 24061

Intrazeolite Rhodium Carbonyl and Rhodium Carbonyl Phosphine Complexes

BRIAN E. HANSON,*[†] MARK E. DAVIS,*[‡] DENNIS TAYLOR,[†] and EDWARD RODE[‡]

Received March 24, 1983

Intrazeolite rhodium carbonyl complexes are readily synthesized by carbon monoxide reduction of rhodium(III)-exchanged zeolites. Although a variety of rhodium carbonyls can be formed within and on the zeolite, the dicarbonyl, $Rh(CO)_2^+$, is the best characterized and easiest to synthesize reproducibly. The reactions of this species with phosphines (P(2-cyanoethyl)$_3$, PPh_3, PMe_2Ph, and $Ph_2PCH_2PPh_2$) over a range of temperatures give insight into the location and mobility of $Rh(CO)_2^+$.

Rhodium-exchanged zeolites have received a great deal of attention in the literature.[1-12] These materials have been studied by infrared spectroscopy,[1-4,8-11] X-ray photoelectron spectroscopy,[5] solution- and gas-phase hydroformylation,[6,7] methanol and ethanol carbonylation,[8-11] and transmission electron microscopy.[12] Although it is difficult to compare independent studies directly owing to different sample preparation and handling techniques, the following general themes seem to be fairly well accepted.

(1) Reduction of Rh(III) to Rh(I) occurs readily at ambient temperatures under low pressures of CO in the presence of water.[3] The most likely process is

$$\mathrm{Rh(III) + CO + H_2O \rightarrow Rh(I) + CO_2 + 2H^+} \quad (1)$$

At very low temperatures, a Rh(III)-CO species has been observed.[3]

(2) The rhodium(I) species formed is usually postulated to be a dicarbonyl complex, $Rh(CO)_2^+$, with the anion not specified (perhaps a framework oxygen). It is speculated that the state of aggregation of rhodium varies from atomic dispersion to rhodium rafts.[11] By analogy to homogeneous systems, $[Rh(CO)_2X]_2$ and $Rh(CO)_2LX$ (L = ligand, X = anion) are likely possibilities. Infrared data for the intrazeolite $Rh(CO)_2^+$ complexes vary according to preparation, with two

---

[†] Department of Chemistry.

[‡] Department of Chemical Engineering.

(1) Gelin, P.; Ben Taarit, Y.; Naccache, C. *J. Catal.* **1979**, *59*, 357.
(2) Primet, M. *J. Chem. Soc., Faraday Trans.* **1978**, *74*, 2570.
(3) Primet, M.; Vedrine, J. C.; Naccache, C. *J. Mol. Catal.* **1978**, *4*, 411.
(4) Worley, S. D.; Rice, C. A.; Mattson, G. A.; Curtis, C. W.; Guin, J. A.; Tarrar, A. R. *J. Phys. Chem.* **1982**, *86*, 2714 and references therein (for rhodium on alumina and related supports).
(5) Andersson, S. L. T.; Scurrell, M. S. *J. Catal.* **1979**, *59*, 340.
(6) Mantovani, E.; Palladino, N.; Zanobi, Z. *J. Mol. Catal.* **1977-1978**, *3*, 285.
(7) Arai, H. *J. Catal.* **1982**, *75*, 188.
(8) Yamanis, J.; Lien, K. C.; Caracotsios, M.; Powers, M. E. *Chem. Eng. Commun.* **1981**, *6*, 355.
(9) Scurrel, M. S.; Howe, R. F. *J. Mol. Catal.* **1980**, *7*, 535.
(10) Yamanis, J.; Yang, K. C. *J. Catal.* **1981**, *69*, 498.
(11) Scurrel, M. S.; Hauberg, T. *Appl. Catal.* **1982**, *2*, 225.
(12) Kaufherr, N.; Primet, M.; Dufaux, M.; Nacchache, C. *C. R. Acad. Sci., Ser. C* **1976**, *286*, 131.

0020-1669/84/1323-0052$01.50/0

to four bands reported in the general regions of 2070–2100 and 2010–2040 cm^{-1}. Observation of more than two bands may indicate slightly different sites at which the complex binds to the zeolite framework. When rhodium-exchanged zeolites are reduced with hydrogen followed by CO adsorption, the appearance of a geminal dicarbonyl appears to be a function of dispersion;[2] the site of adsorption is considered not to be a metallic rhodium atom.

(3) In some preparations, Rh(0) clusters have been observed. These are generally identified by the presence of a triply bridging CO stretch in the infrared spectrum of the intrazeolite complex.[6] The reported preparation of clusters in zeolites requires stringent conditions (130 °C, 80 atm) when rhodium is exchanged into the zeolite as $[Rh(NH_3)_6]Cl_3$. Alternatively, $Rh_6(CO)_{16}$ has been sublimed directly onto Na–Y zeolite.[1]

Rhodium-exchanged zeolites have been investigated as catalysts for two reactions that typically use homogeneous rhodium complexes as catalysts, namely hydroformylation and alcohol carbonylation. The rhodium(I) dicarbonyl precursor formed in situ from the Rh(III) zeolite produces an active catalyst for the gas-phase carbonylation of methanol and ethanol.[8-11] Rhodium clusters formed in situ have also been studied as heterogeneous catalysts for the solution-phase hydroformylation of 1-hexene.[6,13] The supported clusters do not behave substantially differently from the clusters in solution for the hydroformylation of olefins. There has been one report of the gas-phase hydroformylation of propene using an intrazeolite rhodium complex.[7] In this case the nature of the complex is not known.

Within the context of the present work there are certain aspects of the chemistry of rhodium-exchanged zeolites, as reported in the literature, that remain unclear. Most important is the lack of a direct method for establishing whether a particular exchange procedure deposits rhodium only on the surface of a zeolite particle or within the channels and cages of the zeolite structure. Surface spectroscopic techniques such as X-ray photoelectron spectroscopy (XPS) have been used on rhodium-exchanged zeolites to determine the distribution of the metal on the surface vs. the bulk of the zeolite.[5] XPS, however, can alter the nature of the exchanged rhodium. For example, photoreduction of Rh^{3+} has been observed.[5,14] In this paper we present a chemical method specific for the location of rhodium carbonyl complexes synthesized within zeolites. The method involves reaction of the zeolite rhodium carbonyl complexes with phosphines of various sizes and monitoring the infrared spectrum of the metal complex. In the literature, very little attention has been given to the intrazeolite coordination chemistry of rhodium.

Experimental Section

The sodium form of 13X zeolite was obtained from LINDE and had an average particle size of 8 μm. This was pretreated by washing with distilled water and drying in air at 120 °C. At this stage the material is referred to as fully hydrated 13X zeolite. Exchange of Rh(III) into the zeolite was accomplished in one of two ways. First, $RhCl_3 \cdot 3H_2O$ was dissolved in a minimum of boiling ammonium hydroxide solution. After complete dissolution of the rhodium trichloride, the hydrated zeolite was added. The solution was then stirred at room temperature for 24 h.[14] The second method was to dissolve $[Rh(NH_3)_5Cl]Cl_2$ in boiling water followed by addition of the hydrated zeolite. This mixture was maintained at 50 °C for 24 h. The two preparations will be referred to as (1) Rh(OH)–Z and (2) $Rh(NH_3)$–Z. A typical preparation involved 5 g of zeolite and 40 mL of rhodium solution. If complete exchange takes place, the resulting zeolite should contain 1 wt % rhodium. Actual zeolite loadings were determined by acid digestion of the zeolite followed by atomic absorption spectroscopy analysis for rhodium. Weight percent water was determined by TGA.[15] After exchange with rhodium, the samples were washed with distilled water and dried in vacuo at 25 °C. Analytical data are as follows. Rh(OH–Z: 0.78 wt % Rh, 25 wt % H_2O. $Rh(NH_3)$–Z: 0.79 wt % Rh, 25 wt % H_2O.

Table I. Carbonyl Stretching Frequencies for Complexes 1–4 and Some Binary Rhodium Carbonyl Compounds

compd	ν_{CO}, cm^{-1}
$Rh_6(CO)_{16}$ (**1**)	2082 s, 2040 w, 2000 w sh, 1805 s
$Rh_x(CO)_y$ (**2**)	2020 s, 1995 s, 1890 m
$Rh(CO)_2{}^+$ (**3**)	2089 s, 2014 s
$Rh(CO)_w$ (**4**)	2140 sh, 2080 sh, 2030 s, 1978 sh 2346 (CO_2(ads))
$Rh_6(CO)_{16}{}^a$	2070 s, 2040 w, 2020 w, 1800 s
$Rh_4(CO)_{12}{}^b$	2074 s, 2064 s, 2061 m, 2043 ms, 1885 s
$Rh_2(CO)_8{}^c$	2087 s, 2062 s, 1852 m, 1832 m
CO(ads) on Rh metal supported on alumina[d]	2110 s, 2040 s, 2045 s, 1925 m

[a] Reference 6. [b] Beck, W.; Lottes, K. *Chem. Ber.* **1961**, *94*, 2578. [c] Vidal, J. L.; Walker, W. E. *Inorg. Chem.* **1981**, *20*, 249. [d] Yang, A. C.; Garland, C. W. *J. Phys. Chem.* **1957**, *61*, 1504.

Table II. Infrared Data for Products from Carbonylation of $Rh(NH_3)$–Z

compd	ν_{CO}, cm^{-1}
$Rh(CO)_2{}^+$	2099 s, 2017 s
$Rh(CO)_w$ (**6**)	2046 sh, 1987 br
$Rh_x(CO)_y$ (**7**)	2020 s, 2002 s, 1875 sh, 1820 sh

The first preparation, Rh(OH)–Z, was attempted with the thought of generating $[Rh(NH_3)_5Cl]^{2+}$ in situ, which could then exchange into the zeolite. The chemistry of rhodium exchanged into the zeolite by this procedure differs significantly from direct exchange of $[Rh(NH_3)_5Cl]^{2+}$ in aqueous solution (vide infra). The reason for the difference is not clear; one clue may be the fact that the first exchange was performed at high pH. Both preparations show the presence of NH_3 bending modes in the infrared spectrum.

Noncatalytic carbonylations of rhodium zeolites were performed in a Parr minireactor. High-temperature reactions of rhodium carbonyls on zeolite with the phosphines tris(2-cyanoethyl)phosphine and triphenylphosphine were performed by first mixing the solids in a dry nitrogen atmosphere and then heating the mixture to 130 °C, well above the melting point of the phosphine. A partial pressure of carbon monoxide is necessary to prevent total loss of coordinated CO. Ambient-temperature reactions of these phosphines with rhodium carbonyl on zeolite were performed under nitrogen in dry methylene chloride.

Infrared studies were performed on a Nicolet MX-1 Fourier transform infrared spectrophotometer. Samples were prepared as KBr disks in a Vacuum Atmospheres drybox under nitrogen atmosphere. Variations in the KBr-disk preparation technique had no effect on the carbonyl region of the spectrum, indicating that cation exchange within the KBr disks did not interfere with the spectral area of interest, namely the carbonyl stretching region. Infrared spectra of all preparations were also recorded as mulls in mineral oil. These were in no way different in the carbonyl stretching region from the same samples recorded as KBr pellets. Thus, localized heating during the fusion of KBr did not alter the carbonyl species formed under the reaction conditions.

Results and Discussion

Carbonylation of Rh(III) Ion Exchanged Zeolites. The standard reduction potential for $Rh^{III}(aq) \rightarrow Rh^0$ is 0.80 V. Therefore, only very mild reductants are needed to effect this reaction for Rh(III)–Z samples, provided the coordination environment is similar to that of $Rh(H_2O)_6{}^{3+}$. In the absence of stabilizing ligands, rhodium(III) within the zeolite should be reduced to the rhodium metal. Carbon monoxide may act as a reducing agent and stabilizing ligand, yielding rhodium clusters or rhodium(I) dicarbonyl. Spectroscopic evidence for

---

(13) Milledge, A. F. French Patent 1411 602, Dec 17, 1965.

(14) Givens, K. Master's Thesis, VPI & SU, 1982.

(15) Thermogravimetric analysis was performed by E. Yilgor of the Polymer Materials and Interface Laboratory at VPI & SU.

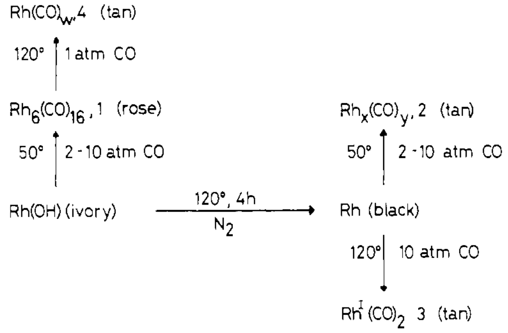

Figure 1. Flow diagram for carbonylation of Rh(OH)–Z.

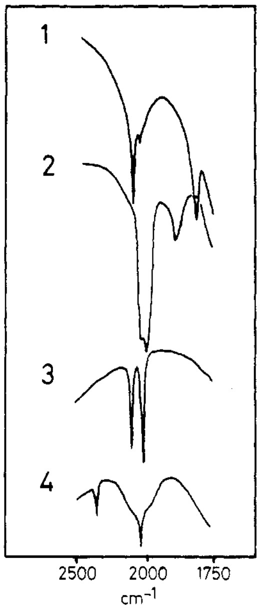

Figure 2. Infrared spectra for intrazeolite complexes **1–4** generated from Rh(OH)–Z.

the formation of these complexes in 13X zeolite is quite convincing.[1-3,8-11] Also, OH^- and NH_4^+ are capable of reducing Rh(III) to rhodium metal.[16]

Figure 1 shows schematically the chemistry for the reactions of Rh(OH)–Z with CO. Figure 2 shows the infrared spectra in the carbonyl region for the zeolitic carbonyl complexes **1–4**. Table I lists the observed stretching frequencies in the carbonyl region. Values for $Rh_6(CO)_{16}$, $Rh_4(CO)_{12}$, $Rh_2(CO)_8$, and CO adsorbed on rhodium are tabulated for comparison.

Comparison of the infrared spectrum of **1** with the reported values for $Rh_6(CO)_{16}$ leads to the assignment of this cluster species to **1**. This is in remarkable contrast to the results of Mantovani et al.,[6] who reports a pressure of 80 atm and a temperature of 130 °C to form rhodium clusters. Starting with Rh(OH)–Z, pressures of only 2 atm are required to form clusters. In our hands, all rhodium-exchanged zeolites give mixtures of products at high temperatures and pressures (Figures 1 and 3).

The rhodium clusters formed on the zeolite are stable for several days under an atmosphere of dry nitrogen. When **1** is heated to 120 °C under 1 atm of CO or N_2, an infrared spectrum is obtained that is consistent with only terminal carbonyls bonded to rhodium. These, however, are not the ubiquitous $Rh(CO)_2^+$. The formulation of **4** as $Rh(CO)_w$ is meant to suggest that a variety of mononuclear rhodium carbonyls are present.

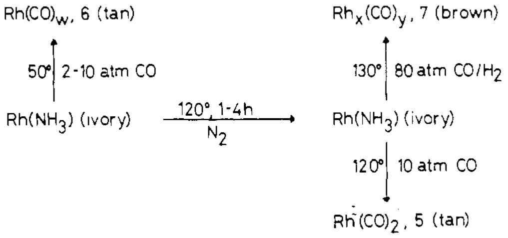

Figure 3. Flow diagram for carbonylation of $Rh(NH_3)$–Z.

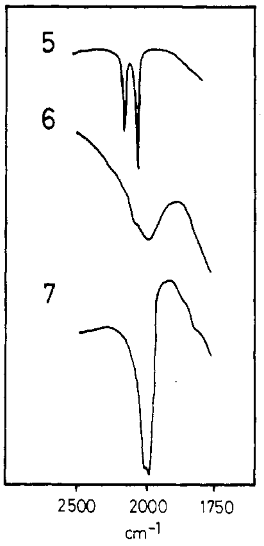

Figure 4. Infrared spectra for intrazeolite complexes **5–7** generated from $Rh(NH_3)$–Z.

When Rh(OH)–Z is heated to 120 °C under N_2, then cooled to 50 °C, and carbonylated with CO, a new spectrum is obtained that differs from that of **1**. The infrared absorption at 1890 cm^{-1} is assigned to a doubly bridging carbonyl. Thus, this complex is designated $Rh_x(CO)_y$ (**2**, $x \geq 2$) to allow for a bridging carbonyl. The presence of bridging carbonyls suggests some aggregation of rhodium, but discrete cluster complexes apparently are not formed. The black color following the temperature pretreatment is consistent with formation of rhodium metal; however, the infrared spectrum of **2** is significantly different from that observed for CO on rhodium metal (see Table I).

After the same temperature pretreatment as for **2**, carbonylation at 120 °C leads clearly to $Rh(CO)_2^+$ (**3**). The dicarbonyl **3** is formed under a variety of conditions in our hands as well as others as reported in the literature.

Carbonylation of $Rh(NH)_3$–Z is qualitatively quite different from that obtained for Rh(OH)–Z (see Figure 3). For example, comparison of the treatments at 50 °C and 2–10 atm of CO for Rh(OH)–Z and $Rh(NH_3)$–Z shows that the former leads clearly to rhodium clusters (most likely $Rh_6(CO)_{16}$ from Table I), while this treatment for the ammine complex leads to a complex of undetermined stoichiometry (**6**). Higher temperatures for both Rh(OH)–Z and $Rh(NH_3)$–Z lead to the composition of $Rh(CO)_2^+$. Although qualitatively these are the same, quantitatively there are some subtle, but real, differences. In particular, the CO stretching frequencies have shifted to higher wavenumber for the ammine precursor (compare **3** and **5**). Although the ratio of ν_{sym}/ν_{asym} for the two preparations seems to have changed, this is apparently an artifact in the spectrum shown. In all other spectra of $Rh^I(CO)_2X$ generated from $Rh(NH_3)$–Z, the relative intensities of ν_{sym}/ν_{asym} are the same as for Rh(OH)–Z (see Figure 5, for example).

The reaction of $Rh(NH_3)$–Z with CO/H_2 at 130 °C and 80 atm was attempted to reproduce the result by Mantovani

---

(16) The oxidation potential for $4OH(aq)^- \rightarrow 2H_2O(l) + O_2(g) + 4e^-$ is −0.40 V. The calculated potential for $2NH^{4+}(aq) \rightarrow 8H^+(aq) + 6e^-$ is −0.27 V.

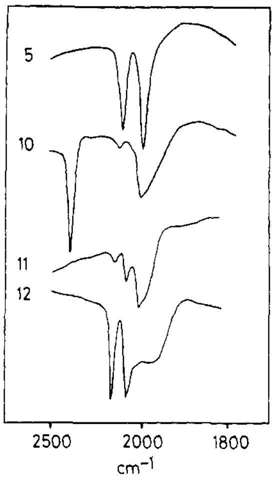

Figure 5. Infrared spectra for intrazeolite rhodium carbonyl phosphine complexes.

et al.[6] of cluster formation from rhodium-exchanged zeolites using ammine complexes. In our hands, cluster formation is not clear-cut. The resulting complex, **7**, appears very similar to **2** from Rh(OH)–Z. An additional shoulder in the spectrum of **7** at 1820 cm^{-1} may indicate the presence of a small amount of $Rh_6(CO)_{16}$. We formulate **2** and **7** as $Rh_x(CO)_y$ where x is at least 2. Thus, the infrared band in **2** at 1890 cm^{-1} and the shoulder at 1875 cm^{-1} in **7** are assigned to a doubly bridging carbonyl. These resutlts are unchanged with use of a variety of pretreatments for $Rh(NH_3)$–Z, including heating in air to 150 °C to dry the sample.

Under the conditions used to prepare **2**, **7** and **4**, **6**, formulated as $Rh_x(CO)_y$ and $Rh(CO)_w$, respectively, it is clear that more than the rhodium carbonyl complex must be responsible for the observed infrared spectra. Complexes **4** and **6** are assigned mononuclear structures due to the lack of bridging carbonyls; w may vary from 1 to 3.

The effect of heating Rh(OH)–Z and $Rh(NH_3)$–Z under N_2 reveals a significant difference in the two materials. The former is much more readily thermally reduced as indicated by the observed color changes.

Reactions of Intrazeolite Rhodium Carbonyls with Phosphines. The question of whether rhodium carbonyls formed by CO reduction are inside the zeolite or on the surface can be addressed directly by observing their reaction with phosphines. It is well-known that, in solution, $[Rh(CO)_2Cl]_2$ reacts readily with triphenylphosphine to give $Rh(CO)(PPh_3)_2Cl$ (eq 2).[17] This reaction proceeds rapidly at room temperature.[18]

$$[Rh(CO)_2Cl]_2 + 4PPh_3 \rightarrow Rh(CO)(PPh_3)_2Cl + 2CO \quad (2)$$

$Rh(CO)_2^+$ (**5**) generated from $Rh(NH_3)$–Z was reacted with a variety of phosphines spanning a range of sizes. The results of these reactions are outlined below. The corresponding infrared spectra are collected in Table III and Figure 5.

The smallest phosphine used was $P(CH_3)_2(C_6H_5)$. A few drops of neat phosphine were added to a Schlenck tube containing $Rh(CO)_2^+$ on zeolite at 25 °C. After 3 h, excess phosphine was removed in vacuo. The infrared spectrum shows complete removal of the bands due to $Rh(CO)_2^+$. These are replaced by a broad absorption at 1988 cm^{-1} and two weak shoulders at 1951 and 1931 cm^{-1}. We interpret these as being due to $Rh(CO)(PMe_2Ph)_x^+$ (**8**) where x = 1, 2, or 3. As in the dicarbonyl, it is assumed that the anion is a framework oxygen. Molecular models suggest that $P(CH_3)_2(C_6H_5)$ should readily pass through the 8-Å channels of 13X zeolite. Thus, this reaction cannot distinguish between intrazeolite $Rh(CO)_2^+$ and surface $Rh(CO)_2^+$. This reaction was also performed in CH_2Cl_2 solution with identical results. Triphenylphosphine and tris(2-cyanoethyl)phosphine both have cross sections larger than 8 Å in their most stable conformations. The latter phosphine, however, can twist into more compact configurations. In solution (CH_2Cl_2 or THF), both of these phosphines fail to react with $Rh(CO)_2^+$ (**5**). This result is consistent with $Rh(CO)_2^+$ residing within the zeolite framework.

Table III. Infrared Data (ν_{CO}, cm^{-1}) for Products from Phosphine Reactions with $Rh(CO)_2^+$

	ν_{CO}, cm^{-1}
$Rh(CO)_2^+$ (**8**) + PMe_2Ph (25 °C)	1988 s, br, 1951 w, sh, 1931 w, sh
$Rh_6(CO)_{16}$ (**9**) + $P(EtCN)_3$ (25 °C)	1963 br
$Rh(CO)_2^+$ (**10**) + $P(EtCN)_3$ (120 °C)	2100 w, 2055 vw, sh, 2015, 2000 s, br
$Rh(CO)_2^+$ (**11**) + PPh_3 (120 °C)	2100 w, 2055 m, 2006 s, 1988 sh
$Rh(CO)_2^+$ (**12**) + $Ph_2PCH_2PPh_2$ (120 °C)	2095 s, 2041 s, 2015 sh, 1975 br
$(\eta^3\text{-}C_3H_5)Rh(CO)(PPh_3)_2$[a]	1938
$ClRh(CO)(PPh_3)_2$[b]	1977
$FRh(CO)(PPh_3)_2$[c]	1971

[a] Brown, C. K.; Mowat, W.; Yagupsky, G.; Wilkinson, G. *J. Chem. Soc. A* **1971**, 850. [b] McCleverty, J. A.; Wilkinson, G. *Inorg. Synth.* **1966**, *8*, 214. [c] Vaska, L.; Peone, J., Jr. *J. Chem. Soc. D* **1971**, 418.

Under the same conditions, **1**, which is thought to contain $Rh_6(CO)_{16}$, reacts readily with $P(EtCN)_3$ at room temperature to give $Rh(CO)(P(EtCN)_3)_x^+$ (**9**) (ν_{CO} 1963 cm^{-1} br). Therefore, it is likely that this complex resides on the surface of the zeolite. Independently, an XPS study of the precursor to **1**, i.e. Rh(OH)–Z, suggests that a small gradient of rhodium concentration exists within a zeolite particle, with slightly larger concentrations near the surface.

At high temperatures even the large phosphines are found to react with $Rh(CO)_2^+$. Typically, a sample of **5** and the solid phosphine were ground with mortar and pestle in a dry nitrogen atmosphere. The mixture was then heated to 120 °C under 1 atm of CO in a stainless-steel autoclave. When the phosphine is $P(EtCN)_3$, a new carbonyl stretch at 2000 cm^{-1} appears. This is assigned to $Rh(CO)(P(EtCN)_3)^+$ (**10**). A small shoulder also appears at 2055 cm^{-1}. When triphenylphosphine is used, new carbonyl bands appear at 2055, 2006, and 1988 cm^{-1}. These could be due to $Rh(CO)(PPh_3)^+$ (**11**) and other complexes. In both these cases, some unreacted $Rh(CO)_2^+$ is evident in the infrared spectra.

Bis(diphenylphosphine)methane, DPM, is a potentially chelating ligand. It reacts with **5** to give a new set of geminal dicarbonyl peaks at 2095 and 2041 cm^{-1} and a broad peak at 1975 cm^{-1}. These are tentatively assigned to $Rh(CO)_2(DPM)^+$ and $Rh(CO)DPM^+$ (**12**). A shoulder at 2015 cm^{-1} suggests again that some $Rh(CO)_2^+$ remains unreacted.

In addition to the intrazeolite rhodium phosphine complexes, Table III lists some model compounds for comparison.

The fact that very large phosphines form complexes with $Rh(CO)_2^+$ at high temperature but not at low temperatures suggests that the dicarbonyl is sufficiently mobile to migrate to the surface of the zeolite particle. The alternative explanation is that at elevated temperatures lattice vibrations in the zeolite allow the bulky phosphines to pass through the channels to form intrazeolite complexes. This is possible in the case of $P(EtCN)_3$ but is very unlikely for PPh_3.

In summary, the reactions of rhodium carbonyls formed on 13X zeolite with phosphines can be used to establish where the complex resides on a zeolite particle. For $Rh(CO)_2^+$, generated from $Rh(NH_3)$–Z, these reactions show that the

---

(17) Cotton, F. A.; Wilkinson, G. "Advanced Inorganic Chemistry", 4th ed.; Wiley-Interscience: New York, 1980.

(18) McCleverty, J. A.; Wilkinson, G. *Inorg. Synth.* **1966**, *8*, 214.

dicarbonyl resides within the zeolite framework. The most likely position is the α cage since the β cage is inaccessible to even the smallest phosphine used, i.e. $P(CH_3)_2(C_6H_5)$. Rhodium clusters **1** generated from Rh(OH)-Z, appear to reside on the surface of the zeolite particle by similar reactions. Gelin et al.[1] and Mantovani et al.[6] conclude that rhodium clusters formed by their methods reside in the α cage. The observed stretching frequencies in their preparations are shifted significantly from those obtained for **1** and for pure $Rh_6(CO)_{16}$ (in particular, the bridging carbonyl frequency is shifted to 1770 cm^{-1}). This may reflect a site for **1** at or near the surface of the zeolite.

The reaction of $Rh(CO)_2^+$ (**5**) with large phosphines at 120 °C establishes that the dicarbonyl is sufficiently mobile to migrate to the surface at this temperature. The large phosphines, particularly triphenylphosphine, are much larger than the channel dimension of 13X.

At this point the differences in carbonylation chemistry of Rh(OH)-Z and $Rh(NH_3)$-Z as outlined in Figures 1 and 3 are not clear. We speculate that the two exchange procedures place rhodium at different sites in the zeolite; this may result from the differences in pH in the two exchange methods.

Acknowledgment. We thank Dr. John Yamanis of Allied Corp. for many helpful discussions concerning this work and Dr. John Dillard for help with the XPS experiments. Financial support for this work was provided by the Jeffress Memorial Trust. E.R. wishes to thank Tennessee Eastman for a predoctoral fellowship.

Registry No. $Rh(CO)_2^+$, 88129-88-8; $Rh(CO)(P(EtCN)_3)^+$, 88129-89-9; $Rh(CO)_2(DPM)^+$, 88129-90-2; $Rh(CO)DPM^+$, 88129-91-3; $Rh_6(CO)_{16}$, 28407-51-4; CO, 630-08-0; H_2, 1333-74-0.

Contribution from the Istituto per lo Studio della Stereochimica ed Energetica dei Composti di Coordinazione,
CNR, 50132 Florence, Italy, and Department of Chemistry, Cornell University, Ithaca, New York 14853

A Molecular Orbital Analysis of the Bonding Capabilities of Carbon Disulfide and Carbon Dioxide toward Transition-Metal Fragments

CARLO MEALLI,*[1a] ROALD HOFFMANN,*[1b] and ARMEL STOCKIS[1c]

Received March 2, 1983

The bonding to transition-metal fragments of heteroallene type molecules such as CS_2 and CO_2 is investigated by using the extended Hückel method. When a linear CX_2 molecule and a transition-metal fragment are brought together, the metal atom can either lie in a direction collinear with the X-C-X vector (end-on approach) or lie perpendicular to it (side-on approach). The possible routes that, departing from these two alternative geometries at the *rendezvous* time, subsequently lead to the η^2 coordination of CX_2 have been traced. The calculations show that the reaction path that starts from end-on is energetically most accessible. The C coordination of CO_2, once observed in a cobalt(I) complex, has been considered, and arguments for the stability of this geometry are presented. The paper also deals with the fluxionality processes found in some complexes and offers suggestions as to how one can interpret some of the reactivities of complexed CO_2 and CS_2 molecules.

The coordination properties of triatomics such as CS_2, CO_2, and COS are interesting, especially from a synthetic viewpoint. The ultimate goal is the activation of carbon dioxide, which is potentially the most abundant source of C_1 chemistry. It may be reasonably expected that the activation process proceeds through transition-metal catalysis. In spite of the great efforts devoted to this field, the ascertained coordination of these molecules to transition metals is limited to a restricted number of compounds.[2]

The big problem is that of magnifying the meager bonding capabilities of these triatomic molecules, an operation which will be ensured of success only if the bonding is understood in detail in terms of simple and useful constructs.

From a theoretical point of view the literature is full of qualitative suggestions as to how one should interpret the electronic structure of these compounds;[3] quantitatively, however the number of MO investigations is very limited.[4] Recently, a very nice MO initio study of the models $(PH_3)_2NiCO_2$ and $(PH_3)_2CuCO_2^+$ has appeared.[5] The authors, after investigating several modes of coordination, confirm the validity of the Chatt-Dewar-Duncanson model for metal-olefin complexes when applied to η^2-bonded carbon dioxide molecules. In particular they underline the contribution of electrostatic terms to the total energy. When the metal atom is positively charged, this term dominates and CO_2 may prefer end-on to side-on coordination. On the basis of the latter argument itself, the extended Hückel method[6] may appear rather inadequate for the interpretation of the bonding in these compounds. However, the relative facility with which the calculations can be repeated and the use of the fragment orbital formalism[7] make the EH method still attractive. In particular, many numerical experiments can be made to learn how a metal fragment and a linear triatomic molecule of the type CX_2 can be brought together. After the initial *rendezvous*, we can follow the possible geometrical rearrangment pathways that lead to the different coordination modes experimentally observed.

Definition of the Geometrical Parameters

It is widely accepted that there are three possible modes of coordination of CS_2 or CO_2 molecules to a single metal function. Detailed structural evidence exists for mode **1**,[8]

---

(1) (a) Istituto Stereochimica. (b) Cornell University. (c) Laboratoire de Chimie Organique, Université de Liege, Liege, Belgium.

(2) See the following review articles, summarizing the most recent literature: (a) Butler, I. S.; Fenster, A. E. *J. Organomet. Chem.* **1974**, *66*, 161. (b) Volpin, M. E.; Kolomnikov, I. S. *Organomet. React.* **1975**, *5*, 313. (c) Yaneff, P. V. *Coord. Chem. Rev.* **1977**, *23*, 183. (d) Kolomnikow, I. S.; Grigoryan, M. Kh. *Russ. Chem. Rev.* (*Engl. Transl.*) **1978**, *47*, 603. (e) Eisenberg, R.; Hendricksen, D. E. *Adv. Catal.* **1979**, *28*, 119. (f) Ibers, J. A. *Chem. Soc. Rev.* **1982**, *11*, 1. (g) Werner, H. *Coord. Chem. Rev.* **1982**, *43*, 165.

(3) (a) LeBozec, H.; Dixneuf, P. H.; Carty, A. J.; Taylor, N. J. *Inorg. Chem.* **1978**, *17*, 2568. (b) Conway, P.; Grant, S. M.; Manning, A. R. *J. Chem. Soc., Dalton Trans.* **1979**, 1920.

(4) (a) Sakaki, S.; Kudou, N.; Ohyoshi, A. *Inorg. Chem.* **1977**, *16*, 202. (b) Demoulim, D.; Pullmann, A. *Theor. Chim. Acta* **1978**, *49*, 161. (c) Ozin, G. A.; Huber, H.; McIntosh, D. *Inorg. Chem.* **1978**, *17*, 1472.

(5) Sakaki, S.; Kitaura, K.; Morokuma, K. *Inorg. Chem.* **1982**, *21*, 760.

(6) Hoffmann, R.; Lipscomb, W. N. *J. Chem. Phys.* **1962**, *36*, 2179, 3489; **1962**, *37*, 2878. Hoffmann, R. *Ibid.* **1963**, *39*, 1397.

(7) (a) Hoffmann, R.; Fujimoto, H.; Swenson, J. R.; Wan, C.-C. *J. Am. Chem. Soc.* **1973**, *95*, 7644. (b) Fujimoto, H.; Hoffmann, R. *J. Phys. Chem.* **1974**, *78*, 1167.

0020-1669/84/1323-0056$01.50/0